Phase stability limit of c-BN under hydrostatic and non-hydrostatic pressure conditions

Jianwei Xiao, Jinglian Du, Bin Wen, Roderick Melnik, Yoshiyuki Kawazoe, and Xiangyi Zhang

View Online   **Export Citation**   **CrossMark**

ARTICLES YOU MAY BE INTERESTED IN

Phase stability limit of c-BN under hydrostatic and non-hydrostatic pressure conditions

Jianwei Xiao,[1] Jinglian Du,[1] Bin Wen,[1,a] Roderick Melnik,[2] Yoshiyuki Kawazoe,[3] and Xiangyi Zhang[1]

[1]*State Key Laboratory of Metastable Materials Science and Technology, Yanshan University, Qinhuangdao 066004, China*
[2]*M²NeT Lab, Wilfrid Laurier University, Waterloo25, 75 University Ave. West, Ontario, Canada N2L 3C5*
[3]*New Industry Creation Hatchery Center, Tohoku University, 6-6-4 Aramaki-aza-Aoba, Aoba-ku, Sendai 980-8579, Japan and Institute of Thermophysics, Siberian Branch of the Russian Academy of Sciences, 1, Lavyrentyev Avenue, Novosibirsk 630090, Russia*

Phase stability limit of cubic boron nitride (c-BN) has been investigated by the crystal structure search technique. It indicated that this limit is ∼1000 GPa at hydrostatic pressure condition. Above this pressure, c-BN turns into a metastable phase with respect to rocksalt type boron nitride (rs-BN). However, rs-BN cannot be retained at 0 GPa owing to its instability at pressure below 250 GPa. For non-hydrostatic pressure conditions, the phase stability limit of c-BN is substantially lower than that under hydrostatic pressure conditions and it is also dramatically different for other pressure mode. © 2014 AIP Publishing LLC. [http://dx.doi.org/10.1063/1.4871897]

I. INTRODUCTION

Cubic zinc blende boron nitride (c-BN) is a superhard material,[1–6] and it has been widely used under high-pressure conditions. Hence the phase stability limit of this material under high pressure conditions is an important issue for theoretical and experimental studies, and some computational works have been performed in attempts to solve this issue. Limited by high pressure experiment conditions, the phase stability limit of c-BN is only performed up to 100 GPa, and existed experimental results shown that c-BN is a stable phase at hydrostatic pressure up to 100 GPa.[2,7,8] The phase stability limit of c-BN is still a challenge for experimental study. On the computational aspect, the phase stability of c-BN usually is studied by comparing the enthalpy of c-BN with the other artificial boron nitride polytypes structures under hydrostatic pressure conditions. For example, Wentzcovitch *et al.*[9] found that c-BN can transform into a thermodynamic metastable phase with respect to rocksalt type boron nitride (rs-BN) at pressure above 1100 GPa. Similar results have been obtained for Christensen[10] and Hromadov's[11] first principles calculations. By investigating the phase transformation paths from c-BN to hexagonal boron nitride (h-BN), wurtzite boron nitride (w-BN) and rhombohedral boron nitride (r-BN), Yu *et al.*[3] found that although c-BN is a thermodynamically metastable phase at pressure above 30 GPa, it cannot be transformed into other phases at room temperature owing to high energy barriers from c-BN to other boron nitride polytypes. Meanwhile, many new artificial boron nitride structures have been constructed,[12,13] and their stability have been compared with c-BN under high pressure.

To study the phase stability limit of c-BN under high pressure, we should find a global minimum energy (GME)

phase under high pressure. At the same time, the phase transformation path and energy barrier from c-BN to the GME phase under high pressure must be studied. Limited by the searching technique for the GME phase, the issue about c-BN stability limit can only be analyzed by comparing the enthalpy of c-BN with some artificial boron nitride polytypes structures. Because the GME phase may not be included in these artificial boron nitride polytypes structures, the searched GME phase by previous method is not credible. Until 2006, some searching methods for GME phase have been developed, such as USPEX[14,15] and CALYPSO,[16–18] they use evolutionary algorithms and particle-swarm optimi-zation (PSO) algorithm, respectively. Both USPEX and CALYPSO can find the GME phase and they have been used successfully in many types of structures studies.[18–21] Therefore, these searching methods provide an opportunity for further investigating the phase stability limit of c-BN. Moreover, a practical high pressure condition is not always hydrostatic pressure.[22] Recent calculated results indicated that cubic diamond's phase stability limit is ∼26 GPa at non-hydrostatic pressure condition, and it is substantially lower than phase stability limit of diamond under static pressure condition (1200 GPa).[23] Owing to the similar crystal structure between c-BN and cubic diamond, it is expected that the phase stability limit of c-BN under non-hydrostatic pressure conditions must be different from that under hydrostatic pressure conditions. To study the phase stability limit of c-BN under hydrostatic and non-hydrostatic pressure conditions, USPEX,[14,15] a searching method for GME phase, has been used in this work. Our results indicated that the phase stability limit of c-BN is ∼1000 GPa under hydrostatic pressure conditions, but in non-hydrostatic pressure conditions, the phase stability limit of c-BN is substantially lower than that under hydrostatic pressure conditions and it also dramatically different from other pressure modes.

a)Author to whom correspondence should be addressed. Electronic mail: wenbin@ysu.edu.cn

TABLE I. Optimized crystallographic data, bond length, mass density (D), energy band gap (Eg), and bulk modulus (B) of different boron nitride polytypes at 0 GPa.

Phase	Space group	Lattice parameters (Å)	Coordinated	D (g/cm^3)	B (GPa)	Eg (eV)	Reference
c-BN	F-43M	a = 3.590	4	3.564	380	4.49	This work
		a = 3.589	4		387		32
		a = 3.620					33
		a = 3.625		3.593		4.4	27
		a = 3.585				4.35	34
		a = 3.615					Expt.[28]
						6.1	35
w-BN	P63MC	a = 2.530, c = 4.186	4	3.552	384	5.031	This work
		a = 2.550, c = 4.2					Expt.[33]
		a = 2.555, c = 4.225		3.587		5.24	27
		a = 2.538, c = 4.179	4		387		32
		a = 2.525, c = 4.182				5	34
h-BN	P63/MMC	a = 2.490, c = 6.561	3	2.3405	22	4.11	This work
		a = 2.494, c = 6.660					Expt.[29]
		a = 2.489, c = 6.561	3		14.09		32
		a = 2.491, c = 6.613				4.04	34
rs-BN	FM-3M	a = 3.482	6	3.903	398	2.11	This work
		a = 3.493					9
sc16-BN	PA-3	a = 4.509	4	3.598	335	4.08	This work
		a = 4.51		3.594	345	4.08	36
p-BN	PMN21	a = 2.525, b = 8.777, c = 4.248	4	3.502	374	5.55	This work
		a = 2.525, b = 8.775, c = 4.247		3.503	403	5.51	12

II. COMPUTATIONAL METHODS

In this work, USPEX package was employed to search for the GME phase for boron nitride compound under hydrostatic pressure range from 0 to 2000 GPa at pressure step of 100 GPa, and a series of unit cell boxes with size of 2, 4, 8, 16, and 20 atoms were used, respectively. It is found that the searched GME phases of these different unit cells are consistent with each other. After searching the GME phase, lattice parameters, atom positions, and enthalpy of the searched GME phase combined with the other boron nitride polytypes both under hydrostatic and non-hydrostatic pressure conditions have been calculated by using the first principles method. In this calculation, density functional theory (DFT) based on a plane wave pseudo-potential technique implemented in the CASTEP package[24] has been used, and the interactions between the ions and valence electrons were modeled by the ultra-soft pseudo-potentials (USPP).[25] The exchange and correlation interactions have been described in the local density approximation (LDA-CAPZ).[26] The kinetic cutoff energy for plane waves was set as 770 eV. The k point separation in Brillouin zone was $8 \times 8 \times 8$ for c-BN, rs-BN, and bc8-BN, $12 \times 12 \times 5$ for h-BN, $11 \times 7 \times 9$ for p-BN, and $11 \times 11 \times 4$ for w-BN, respectively. The total energy was converged numerically to 5×10^{-7} eV/atom with respect to electronic, ionic, and unit cell degrees of freedom. The LDA method has been used in this work, given that it can give a reasonable interlayer distances and mechanical properties of h-BN compared with the generalized gradient approximation (GGA).[27] In addition, our benchmark calculations are conducted for c-BN phase, the calculated lattice constant of
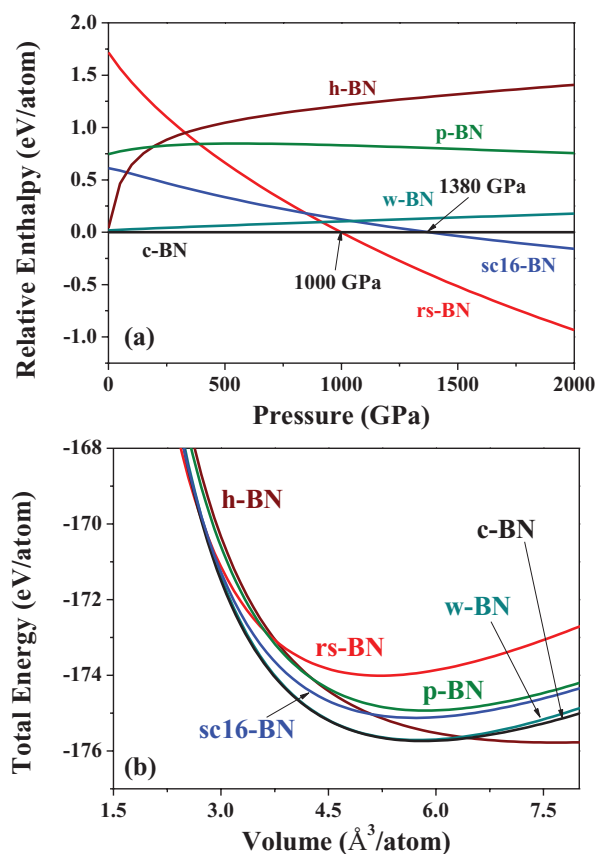

FIG. 1. (a) Enthalpy of rs-BN, sc16-BN, w-BN, p-BN, and h-BN relative to c-BN under hydrostatic pressure. (b) Total energy versus volume for c-BN, rs-BN, sc16-BN, w-BN, p-BN, and h-BN, where the curves are fitted by using Murnaghan's equation of state.[39]

3.592 Å agrees well with the experimental value of 3.615 Å;[28] meanwhile, the lattice parameter c and bulk modulus B for h-BN are 6.561 Å and 22 GPa, and they are in good agreement with the experimental value of 6.660 Å[29] and 37 GPa,[30] respectively. These results confirm that our present computational scheme is reliable.

III. RESULTS AND DISCUSSION

By searching GME phase, two boron nitride polytypes have been found: c-BN (at pressure below 1000 GPa) and rs-BN (at pressure above 1000 GPa). Because c-BN is the experimentally stable phase of boron nitride at pressure above ~15 GPa,[6] it is earthy that c-BN was found in our searching results, this confirms that the reliability of GME phase searching method. For the rs-BN phase, found in our searching results at pressure above 1000 GPa, we observe that the rs-BN is a thermodynamically stable phase at pressure above 1000 GPa. This result also implies that the stability limit of c-BN under hydrostatic pressure conditions may be ~1000 GPa, and it agrees with Wentzcovitch, Christensen and Hromadov's results.[9–11] For comparative study, the other four BN polytypes (namely, w-BN, h-BN, p-BN, and sc16-BN) combined with c-BN and rs-BN have been built by using crystallographic data from Refs. 12 and 31. The calculated crystallographic parameters and bulk modulus for the six boron nitride polytypes are listed in Table I. As can be seen that the obtained lattice parameters for the six BN polytypes agree

well with the experimental and previously reported theoretical results.[9,27–29,32–36] There is one type of bonds for both c-BN and rs-BN, and the bond lengths of B-N are 1.556 Å and 1.741 Å for c-BN and rs-BN, respectively. The calculated bulk modulus of rs-BN is 398 GPa, and it is larger than c-BN bulk modulus of 384 GPa. Although the bond length of c-BN is shorter than that of rs-BN, the mass density of rs-BN (3.903 g/cm^3) is larger than that of c-BN (3.564 g/cm^3), owing to the fact that the coordinated number of rs-BN (6) is larger than that of c-BN (4). Therefore, the bulk modulus of rs-BN is larger than that of c-BN due to the increased mass density. For the same reason, the bulk modulus of c-BN is larger than bulk modulus of p-BN (374 GPa). Besides, the calculated energy band gap indicated all of these BN polytypes are wide band gap semiconductor under ambient conditions.

To further analyze the thermodynamic stability of these six boron nitride polytypes, the lattice parameters and atomic positions of these boron nitride polytypes under pressure up to 2000 GPa have been optimized, and the corresponding enthalpies of these optimized boron nitride polytypes have been obtained. The enthalpies per atom for rs-BN, sc16-BN, h-BN, p-BN, and w-BN as functions of pressure related to c-BN are plotted in Figure 1(a). The results indicated that the c-BN is the thermodynamically stable phase at pressure below 1000 GPa, and rs-BN becomes the thermodynamically stable phase at pressure above 1000 GPa. This result is consistent with our searched GME phases and experimental result on phase stability of c-BN.[2,7,8] The w-BN, h-BN, and p-BN are still thermodynamically metastable phases respect
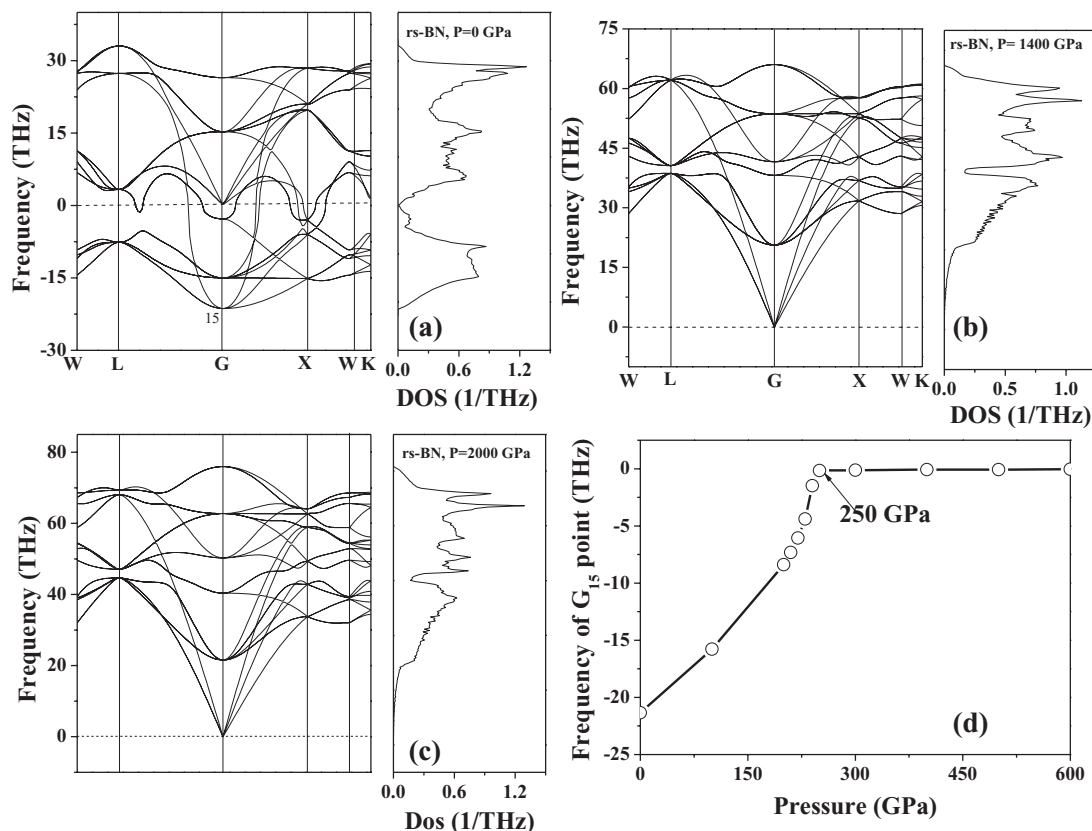

FIG. 2. Calculated phonon band structure and density of states of rs-BN at pressures of 0 GPa (a), 1400 GPa (b), and 2000 GPa (c). (d) The frequency of G_{15} point at different pressures.

to c-BN. Unlike the corresponding carbon polytypes,[37,38] sc16-BN is still a metastable phase with respect to c-BN or rs-BN at the pressure ranges studied here. Correspondingly, the curves of the total energy as a function of volume are plotted in Figure 1(b). These curves have been fitted by using Murnaghan's equation of state structure,[39] which is consistent with the enthalpies-pressure relationships as shown in Figure 1(a).

The dynamically stability of these six boron nitride polytypes has been studied by calculating their phonon band structure. This phonon band structure and density of states are plotted in Figure 2 and Figure 1 of the supplementary material.[40] As shown in Figure 2, rs-BN is not a dynamically stable phase at pressure below 250 GPa. Therefore, although rs-BN is a stable phase at pressure above 1000 GPa, it cannot retain stability at 0 GPa. Based on the calculated phonon band structure, c-BN is dynamically stable until the pressure is above of 2720 GPa.

To further explore the mechanical stability of c-BN under hydrostatic pressures, the Born stability criteria and special deformations have been considered in this work. For a cubic lattice under the hydrostatic pressure of P, the Born stability criteria can be expressed as formula (1):[41]

$$C_{11} + C_{12} + 2P > 0, \quad C_{11} - C_{12} - P > 0, \quad C_{44} - P/2 > 0,$$
$$(1)$$

where the C_{ij} denotes the elastic constants. The calculated $C_{44} - P/2$ and $C_{11} - C_{12} - P$ as a function of pressure for c-BN are depicted in Figure 2 of the supplementary material.[40] As is reflected that the $C_{44} - P/2$ increases with the increase of pressure; while the $C_{11} - C_{12} - P$ decreases with the increase of pressure, and the $C_{11} - C_{12} - P$ equals to zero when the pressure reached at 1150 GPa. These results indicated that the c-BN is tetragonal shear unstable when pressure is above 1150 GPa. In addition, the mechanical stability of cubic lattice can be estimated from the viewpoint of special deformations, i.e., the cubic phase is considered mechanically stable when the total energy curves contain the minimum value under the isotropic, tetragonal, and trigonal deformations.[42] Accordingly, the total energy curve for c-BN as a function of isotropic, tetragonal, and trigonal deformations at 0 and 3000 GPa have been plotted in Figure 3 of the supplementary material.[40] The results indicated that c-BN is mechanically stable at 0 and 3000 GPa; while it will become mechanically unstable at higher pressures due to the fact that the total energy curve under tetragonal deformation softens with the increase of pressure, as is reflected in Figure 3(b) of the supplementary material.[40]

As mentioned above, the stability limit of c-BN is different from the viewpoints of dynamical and mechanical stability criteria. Even so, all of these results indicated that c-BN is unstable and will transform into other stable BN polytypes under high hydrostatic pressure conditions.

Because the stability limit of c-BN under hydrostatic pressure cannot be explained just by using the enthalpies-pressure relationships. To better study stability limit of c-BN under hydrostatic pressure and its atomic mechanism of phase transformation between c-BN and rs-BN, the phase transition paths between c-BN and rs-BN has been investigated at dif-
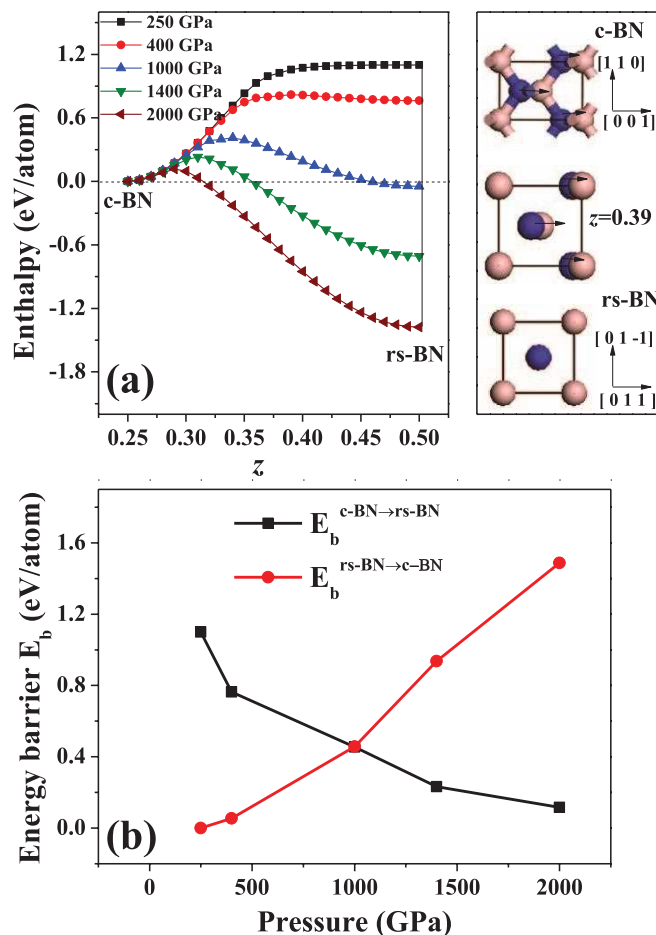

FIG. 3. The calculated phase transformation paths between c-BN and rs-BN (a) and the phase transformation energy barrier between c-BN and rs-BN under hydrostatic pressure (b).

ferent pressure values (250, 400, 1000, 1400, and 2000 GPa). To build the phase transformation path, a series of intermediate structures have been built. These intermediate structures are orthorhombic lattices, and their unit cells include four atoms with fractional coordinates of B1 (0, 0, 0), B2 (0.5, 0.5, 0.5), N1 (0, 0.5, z), and N2 (0.5, 0, 0.5 + z), respectively.[43] The z value ranging from 0.25 to 0.5 is regarded as an intermediate parameter. For z = 0.25, the structure is c-BN. For z = 0.5, the structure is rs-BN. Each intermediate structure has been fully relaxed at given pressures by fixing the fractional coordinates of atoms, and finally the enthalpies have been obtained. They are plotted in Figure 3. As shown in Figure 3, with increasing pressure, the energy barrier from c-BN to rs-BN decreases monotonously. When the pressure is 1000 GPa, the energy barrier from c-BN to rs-BN is ∼0.4 eV/atom. It is clear that in this case the phase transition from c-BN to rs-BN cannot happen at room temperature, and more external energy is needed to overcome this high energy barrier. These results mean that the phase stability limit of c-BN is larger than 1000 GPa at room temperature. When the hydrostatic pressure reaches 2000 GPa, the energy barrier from c-BN to rs-BN is about 0.11 eV/atom. This result implies that when the pressure is larger than 2000 GPa, the c-BN can transform into rs-BN at room temperature. For the phase transition energy barrier from rs-BN to c-BN, when hydrostatic pressure is less
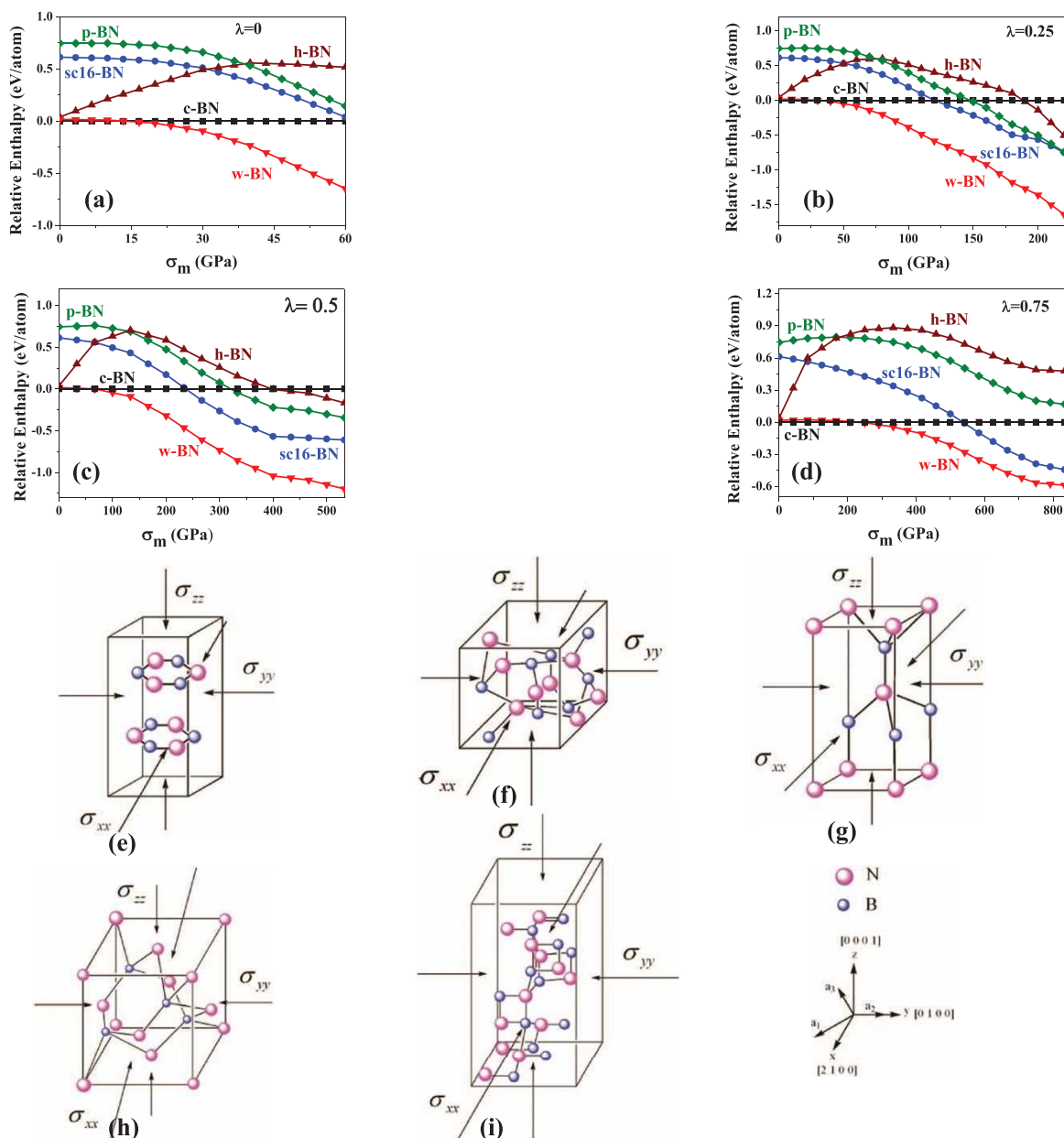
FIG. 4. The mean pressure dependent relative enthalpies of sc16-BN, h-BN, p-BN, and w-BN with respect to c-BN under non-hydrostatic pressure condition at different λ: (a) λ = 0, (b) λ = 0.25, (c) λ = 0.5, and (d) λ = 0.75. The schematic diagrams of non-hydrostatic compressing model for h-BN (e), sc16-BN (f), w-BN (g), c-BN (h), and p-BN (i), respectively.

than 250 GPa, energy barrier from rs-BN to c-BN is zero. This result is consistent with the result on dynamically instability of rs-BN at pressure below 250 GPa. Therefore, although the c-BN can transform into rs-BN under high hydrostatic pressure, the rs-BN cannot be preserved at pressure below 250 GPa. When hydrostatic pressure is larger than 250 GPa, the energy barrier from rs-BN to c-BN increases monotonously. When hydrostatic pressure reaches 2000 GPa, the energy barrier from rs-BN to c-BN is about 1.49 eV/atom.

To investigate the phase stability limit of c-BN under non-hydrostatic pressure conditions, the enthalpies of c-BN with the other four boron nitride polytypes (w-BN, sc16-BN, p-BN, and h-BN) have been compared. In this work, the non-hydrostatic pressure conditions are considered as $\sigma_{xx} = \sigma_{yy} = \lambda\sigma_{zz}$, where $\sigma_{xx}, \sigma_{yy}, \sigma_{zz}$ are axial stress in x, y, z directions

respectively, and λ is a variable parameter. The mean stress is calculated by $\sigma_m = (\sigma_{xx} + \sigma_{yy} + \sigma_{zz})/3 = (2\lambda + 1)\sigma_{zz}/3$. The schematic diagrams for boron nitride polytypes under non-hydrostatic pressure conditions are presented in Figures 4(e), 4(f), and 4(i). For w-BN and h-BN, σ_{zz} is parallel to [0001] direction of hexagonal lattice, but for c-BN, p-BN, and sc16-BN, σ_{zz} is parallel to [001] direction of cubic lattice. In this work, four non-hydrostatic pressure conditions (with λ = 0, 0.25, 0.5 and 0.75) have been considered. The lattice parameters of these four boron nitrides have been optimized, and the corresponding enthalpies have been calculated. The relationships between enthalpies of boron nitride polytypes and σ_m under different non-hydrostatic pressure conditions are plotted in Figures 4(a)–4(d). The results indicated that the critical value of σ_m for thermodynamically stable phase to

be converted from c-BN to w-BN is 16.67, 30, 66.67, and 208.33 GPa which correspond to $\lambda = 0$, 0.25, 0.5, and 0.75, respectively. The critical value of σ_m is below the safety limit compressive strength of w-BN,[44] and the critical value of σ_m increases with the increase of λ. Compared to the phase stability limit of c-BN under hydrostatic pressures, the phase stability limit of c-BN under non-hydrostatic pressures is substantially lower.

The phase transformation path between c-BN and w-BN has been investigated under different non-hydrostatic pressure conditions. To build the phase transformation path, a series of intermediate structures have been built. The space group of these intermediate structures are fixed as PCA21, and four atoms with fractional coordinates of B1 ($-0.917 - 0.333\xi$, $0.125 - 0.125\xi$, $0.9375 - 0.25\xi$), B2 ($-0.417 - 0.083\xi$, $0.375 + 0.125\xi$, 0.9375), N1 ($-0.917 - 0.083\xi$, $0.125 - 0.125\xi$, 0.5625) and N2 ($-0.417 - 0.333\xi$, $0.375 + 0.125\xi$, $0.5625 \ 0.25\xi$) are added. The ξ value ranging from 0 to 1 is regarded as an intermediate parameter. For $\xi = 0$, the structure is w-BN. For $\xi = 1$, the structure is c-BN. Each intermediate structure has been fully relaxed at seven non-hydrostatic pressures conditions (with $\lambda = -0.25$, 0, 0.25, 0.5, 0.75, 1.0, and 1.25) by fixing the fractional coordinates of atoms, and the corresponding enthalpies have been calculated and they are plotted in Figure 4 of the supplementary material.[40] The phase transformation energy barrier from c-BN to w-BN is ~1.62 eV/atom at 0 GPa, and it increases with the increase of mean pressure. Although c-BN becomes the thermodynamically metastable phase with respect to w-BN at mean pressure above critical value under non-hydrostatic pressure condition, it cannot be transformed into w-BN at room temperature, since an external energy is needed to overcome a higher energy barrier.

IV. CONCLUSIONS

In summary, the phase stability limits of c-BN under both hydrostatic and non-hydrostatic pressure conditions have been investigated by the crystal structure search technique. The results indicated that under hydrostatic pressure condition, the phase stability limit of c-BN is about 1000 GPa; and c-BN will become a metastable phase with respect to rs-BN when the pressure is higher than this critical pressure. Our results also found that rs-BN is an unstable phase at pressure below 250 GPa. Under non-hydrostatic pressure condition, the phase stability limit of c-BN is tightly related to the compressing modes, and the corresponding critical phase stability transformation mean pressure from c-BN to w-BN is 16.67, 30, 66.67, and 208.33 GPa at $\lambda = 0$, 0.25, 0.5, and 0.75, respectively.

ACKNOWLEDGMENTS

[1] Y. Zhang, H. Sun, and C. Chen, Phys. Rev. Lett. **94**, 145505 (2005).

[2] F. Datchi and B. Canny, Phys. Rev. B **69**, 144106 (2004).

[3] W. Yu, W. Lau, S. Chan, Z. Liu, and Q. Zheng, Phys. Rev. B **67**, 014108 (2003).

[4] J. Liu, Y. Vohra, J. Tarvin, and S. Vagarali, Phys. Rev. B **51**, 8591 (1995).

[5] J. MacNaughton, A. Moewes, R. Wilks, X. Zhou, T. Sham, T. Taniguchi, K. Watanabe, C. Chan, W. Zhang, I. Bello, S. Lee, and H. Hofsäss, Phys. Rev. B **72**, 195113 (2005).

[6] Y. Tian, B. Xu, D. Yu, Y. Ma, Y. Wang, Y. Jiang, W. Hu, C. Tang, Y. Gao, K. Luo, Z. Zhao, L. M. Wang, B. Wen, J. He, and Z. Liu, Nature (London) **493**, 385 (2013).

[7] T. Kawamoto, K. N. Matsukage, T. Nagai, K. Nishimura, T. Mataki, S. Ochiai, and T. Taniguchi, Rev. Sci. Instrum. **75**, 2451 (2004).

[8] N. Funamori and T. Sato, Rev. Sci. Instrum. **79**, 053903 (2008).

[9] R. Wentzcovitch, M. Cohen, and P. Lam, Phys. Rev. B **36**, 6058 (1987).

[10] N. Christensen and I. Gorczyca, Phys. Rev. B **50**, 4397 (1994).

[11] L. Hromadová and R. Martoňák, Phys. Rev. B **84**, 224108 (2011).

[12] X. Jiang, J. Zhao, and R. Ahuja, J. Phys.: Condens. Matter **25**, 122204 (2013).

[13] S. Zhang, Q. Wang, Y. Kawazoe, and P. Jena, J. Am. Chem. Soc. **135**, 18216 (2013).

[14] C. H. Hu, A. R. Oganov, Q. Zhu, G. R. Qian, G. Frapper, A. O. Lyakhov, and H. Y. Zhou, Phys. Rev. Lett. **110**, 165504 (2013).

[15] X. F. Zhou, A. R. Oganov, G. R. Qian, and Q. Zhu, Phys. Rev. Lett. **109**, 245503 (2012).

[16] Q. Li, D. Zhou, W. Zheng, Y. Ma, and C. Chen, Phys. Rev. Lett. **110**, 136403 (2013).

[17] L. Zhu, H. Wang, Y. Wang, J. Lv, Y. Ma, Q. Cui, Y. Ma, and G. Zou, Phys. Rev. Lett. **106**, 145501 (2011).

[18] Y. Xie, A. R. Oganov, and Y. Ma, Phys. Rev. Lett. **104**, 177005 (2010).

[19] Z. Zhao, B. Xu, X. F. Zhou, L. M. Wang, B. Wen, J. He, Z. Liu, H. T. Wang, and Y. Tian, Phys. Rev. Lett. **107**, 215502 (2011).

[20] H. Liu and Y. Ma, Phys. Rev. Lett. **110**, 025903 (2013).

[21] Y. Wang, J. Lv, L. Zhu, and Y. Ma, Comput. Phys. Commun. **183**, 2063 (2012).

[22] X. Luo, Z. Liu, B. Xu, D. Yu, Y. Tian, H. T. Wang, and J. He, J. Phys. Chem. C **114**, 17851 (2010).

[23] B. Wen, M. J. Bucknum, J. Zhao, X. Guo, and T. Li, Diamond Relat. Mater. **17**, 1353 (2008).

[24] S. J. Clark, M. D. Segall, C. J. Pickard, P. J. Hasnip, M. I. Probert, K. Refson, and M. C. Payne, Z. Kristallogr. **220**, 567 (2005).

[25] D. Hamann, M. Schlüter, and C. Chiang, Phys. Rev. Lett. **43**, 1494 (1979).

[26] D. M. Ceperley, Phys. Rev. Lett. **45**, 566 (1980).

[27] C. He, L. Sun, C. Zhang, X. Peng, K. Zhang, and J. Zhong, Phys. Chem. Chem. Phys. **14**, 10967 (2012).

[28] R. H. Wentorf, J. Chem. Phys. **26**, 956 (1957).

[29] Y.-N. Xu and W. Ching, Phys. Rev. B **44**, 7787 (1991).

[30] G. Kern, G. Kresse, and J. Hafner, Phys. Rev. B **59**, 8551 (1999).

[31] A. Mujica, A. Rubio, A. Munoz, and R. Needs, Rev. Mod. Phys. **75**, 863 (2003).

[32] B. Wen, J. Zhao, R. Melnik, and Y. Tian, Phys. Chem. Chem. Phys. **13**, 14565 (2011).

[33] F. P. Bundy and R. H. Wentorf, J. Chem. Phys. **38**, 1144 (1963).

[34] R. Ahmed, S. J. Hashemifar, and H. Akbarzadeh, Physica B: Condensed Matter **400**, 297 (2007).

[35] K. Lawniczak-Jablonska, T. Suski, I. Gorczyca, N. Christensen, K. Attenkofer, R. Perera, E. Gullikson, J. Underwood, D. Ederer, and Z. L. Weber, Phys. Rev. B **61**, 16623 (2000).

[36] X. G. Luo and W. H. Wang, Highlights of Sciencepaper Online **6**, 847 (2013).

[37] M. Yin, Phys. Rev. B **30**, 1773 (1984).

[38] J. Sun, D. D. Klug, and R. Martonak, J. Chem. Phys. **130**, 194512 (2009).

[39] F. D. Murnaghan, Am. J. Math. **59**, 235 (1937).
[40] See supplementary material at http://dx.doi.org/10.1063/1.4871897 for "phase stability limit of c-BN under hydrostatic and non-hydrostatic pressure conditions."
[41] B. Karki, G. Ackland, and J. Crain, J. Phys.: Condens. Matter **9**, 8579 (1997).
[42] B. Wen, S. Takami, Y. Kawazoe, and T. Adschiri, Physica B **406**, 2654 (2011).
[43] M. Y. Lü, Z. W. Chen, L. X. Li, R. P. Liu, and W. K. Wang, Acta Phys. Sin. **55**, 3576 (2006).
[44] Z. Pan, H. Sun, Y. Zhang, and C. Chen, Phys. Rev. Lett. **102**, 055503 (2009).